Author version of : Deep Sea Research Part I: Oceanographic Research Papers, vol.139; 2018; 43-54

New to total primary production ratio (f-ratio) in the Bay of Bengalusing isotopic composition of suspended particulate organic carbonand nitrogen

C.K. Sherin[1], V.V.S.S. Sarma[1]*, G.D. Rao[1], R. Viswanadham[1], M.M. Omand[2] and V.S.N. Murty[1]

[1]CSIR-National Institute of Oceanography Regional Centre,
176 Lawsons Bay Colony, Visakhapatnam, India
[2]Graduate School of Oceanography, University of Rhode Island,
Narragansett, RI 02882, USA
* Corresponding author

Abstract

Variations in the content and isotopic compositions of carbon and nitrogen in the suspended particulate matter were analysed to identify sources of nutrients and compute *f*-ratios (ratio of new production to primary production) in the Bay of Bengal (BoB) during the post-monsoon period (November-December, 2013). Remote sensing data during our observation period indicated that the study region encompassed meso-scale cyclonic (CE) and anticyclonic eddies (ACE) and was influenced by tropical cyclone *Madi* between 6 and 12 December, 2013. Relatively higher concentrations of nitrate were observed in the CE and in the cyclone-influenced region compared to that in the ACE. Variable concentrations of nutrients controlled the size distributions of phytoplankton. Overall, the picoplankton population dominated, but the contributions of micro- and nano-plankton populations were significantly higher in the CE region because of higher concentration of nutrients. The $\delta^{13}C_{sus}$, C:N molar ratios and C:Chl-*a* ratios suggested that suspended matter is mainly contributed by *in situ* processes during the study period. The $\delta^{15}N_{sus}$ of suspended matter suggested that vertical supply of nutrients brought from subsurface water supported new production in the CE and cyclone-influenced regions, whereas regenerated nutrients supported phytoplankton production in the ACE. The *f*-ratios computed using $\delta^{15}N_{sus}$ and depth of nitracline were high in the CE (0.41±0.14) and cyclone-influenced region (0.54±0.12) and lower in the ACE (0.27±0.06). This study revealed that the meso-scale CEs are more important in enhancing exportable production in the BoB. As more than 30 CEs form annually in the BoB, their impact on basin-wide new production and export flux to the deeper ocean must be evaluated using both observations and high-resolution models.

1. Introduction

Lower primary production occurs in the Bay of Bengal (BoB) during southwest monsoon (June to September) due to strong salinity stratification driven by high river discharge (UNESCO, 1979; Krishna et al., 2016) and weaker nutrient inputs through vertical mixing (Rao et al., 1994; Prasanna Kumar et al., 2002; 2004) . In addition to this, shallow photic depth resulting from weak solar radiation due to cloudiness and high suspended matter, further decrease primary production during the southwest monsoon period (Gomes et al., 2000; Madhupratap et al., 2003). In contrast, higher primary production was noticed in the BoB, almost to equivalent level to that of the Arabian Sea, during post-monsoon and winter seasons (October to February). However, potential sources of nutrients supporting such high production during post-monsoon and winter seasons are not clearly known (Gauns et al., 2005). Prasanna Kumar et al. (2002) suggested that cyclonic eddy-driven nutrient supply significantly enhances the phytoplankton biomass in the BoB during the post-monsoon and winter seasons. Based on sediment trap observations and satellite remote sensing data, Vidya and Prasanna Kumar (2013) estimated that ~42 % of the biogenic flux from the northern and central Bay is supported by eddy-driven nutrient supply. Ittekkot et al. (1991) reported higher sinking carbon fluxes to the deep (~3000 m) ocean in the BoB than elsewhere in the world (Jahnke, 1996; Sarma et al., 2006) and attributed high flux to the ballasting of organic matter by river-borne mineral particles. Though the impact of river discharge can be noticed only in the northern BoB, where peak riverine discharge coincides well with the sinking carbon flux, no such correlation was observed in the central and southern BoB (see Figure 2 of Ittekkot et al., 1991). Thus it is argued that the mineral ballast hypothesis applies only for the northern BoB while higher sinking carbon fluxes in the central and southern BoB result from new production supported by physical processes (Sarma et al., 2016).

Recently Anand et al. (2017) found that <2 % of the primary production is sinking to depths deeper than 100 m in the BoB due to dominant heterotrophy in the upper ocean. On the other hand, export flux of 2-10 % has been noted in the Arabian Sea at the depth of 100 m (Buesseler et al., 1998; Anand et al. 2018). The estimated *f*-ratios using enriched nitrogen tracer incubation experiments are found to be similar in both the BoB (0.54-0.72; Kumar et al., 2004a; Kumar and Ramesh, 2005; Gandhi et al., 2010a) and the Arabian Sea (0.15- 0.82; McCarthy et al., 1999; Gandhi et al., 2010b). The incompatibility between *f*-ratios and sinking carbon fluxes in the two basins could arise from incubation artefacts, such as recycling of tracer, bottle effect and duration of the incubation experiment. Besides, the ^{15}N-labelled tracer experiments often provide a measure of uptake potential rather than *in situ* rates due to significant changes in nitrate concentration particularly when ambient concentrations of nitrate are low. The objective of this study is to (1) quantify sources of organic

matter in the mixed layer, (2) examine the sources of nutrients supporting primary production, (3) estimate *f*-ratios using $\Box^{15}N_{sus}$, and (4) evaluate how cyclonic eddies (CE) and anticyclonic eddies (ACE) influence *f*-ratios in the BoB during the post- monsoon season (November – December, 2013).

2. Material and Methods

2.1. *Study area*

Water samples were collected at 32 hydrographic stations along the track of the *RV Roger Revelle* in the BoB during 29 November -12 December 2013 to examine the spatial variations in isotopic composition of carbon and nitrogen in the suspended particulate matter. Sampling stations covered the central BoB between 6^o-18^{o}N and 83^o-90^{o}E. The cruise track was designed to sample various physical regimes- such as highly stratified region (stations-29-36), cyclone-influenced region (47-55), CE region (14-23), strong ACE region (25-45) and weak ACE region (ACE_w; 66-73)- to examine the impacts on sources of nutrients and *f*-ratios in the BoB (Fig. 1).

2.2. *Sampling and Measurements*

Vertical profiles of temperature, salinity (CTD, Sea Bird Electronics, USA), fluorescence (Wet Labs, USA) and dissolved nitrate (SUNA, Satlantic, USA) were measured at 1 m intervals using sensors attached to CTD-Rosette system. Water samples were collected at standard depths in the upper 100 m using 20 L Niskin bottles fitted to the rosette system. Samples for particulate organic matter were collected at surface only. About 5-10 L of water samples were filtered through a 0.7 □m GF/F filter, and the pigments retained on the filter were extracted into 90 % acetone and measured by High Performance Liquid Chromatography (HPLC; 1200 series, Agilent Technologies, USA). Following the method of Grasshoff et al. (1983), nutrients concentrations in the water samples were measured colorimetrically. Both fluorescence based Chlorophyll–*a* (Chl-*a*) and SUNA derived dissolved nitrates were calibrated against the results of using discrete water samples analysis by HPLC and colorimety, respectively. Strong linear correlation between SUNA and colorimetric nitrate (r^2=0.93; $p<0.001$) and between fluorescence and HPLC Chl-*a* (r^2=0.88; $p<0.001$) were noted. The depth of nitracline was derived from the SUNA nitrate profiles and identify by a sharp increase in nitrate concentration. Suspended matter was collected by filtering about 20-30 L of water samples through pre-combusted 0.7 □m GF/F filters (47 mm diameter; Whatman combusted at 300^o C for 6 h) and the filters were stores at -20^{o}C on board. In the shore laboratory, the filters were dried overnight at 50^{0}C and an aliquot of the filter was acid-fumed for 12 h to remove inorganic carbon, and then dried again for analyses of the organic carbon content and isotopic composition. The other aliquot was not

acidified for analyses of nitrogen content and isotopic composition as this treatment alters N isotope values (Goering et al., 1990; Bunn et al., 1995; Pinnegar and Polunin, 1999).

The contents and isotopic compositions of carbon and nitrogen in the suspended matter were measured with an elemental analyser coupled with an Isotopic Ratio Mass Spectrometer (IRMS, Delta V Plus, Thermo Electron, Germany) and the results are expressed relative to conventional standards, i.e., Pee Dee Belemnite (PDB) for carbon (Coplen, 1966) and atmospheric N_2 for nitrogen (Mariotti, 1983) and reported in the "□" notation:

$$\square R = ((X_{sample} - X_{standard})/X_{standard}) \times 10^3 \text{ ------- (1)}$$

where R=^{13}C or ^{15}N and X = $^{13}C/^{12}C$ or $^{15}N/^{14}N$. Tanks of high-purity CO_2 and N_2 were used as working standards. These gases were calibrated with internal reference materials of Glutamic Acid, Alanine, and marine sediment, as well as International Atomic Energy Agency (IAEA) standards. The long-term precision for the instrument is approximately ±0.2‰ for both □^{13}C and □^{15}N.

2.3. Phytoplankton size classes

The pigment biomarkers were grouped to assess the contribution of different size classes to total phytoplankton biomass following Uitz et al. (2006). The sum of all weighted diagnostic pigments (ΣDPw) was calculated as follows:

ΣDPw=1.41 [fuco]+1.41[per]+1.27[19'HF]+0.35[19'BF]+0.60 [allo]+1.01[Chl-*b*]+0.86 [zea] --- (2)

ΣDPw represents the total Chl-a concentration which denotes the total phytoplankton biomass. Where [fuco], [per], [19'HF], [19'BF], [allo], [chl-*b*] and [zea] denote diatoms, dinoflagellates, prymnesiophytes, crysophytes, cryptophytes, chlorophytes and cyanobacteria respectively.

The fractional contribution of different size classes contributing to the total phytoplankton biomass (f_{micro}, f_{nano} *and* f_{pico}) was then derived using the following ratios.

f_{micro} = (1.41 [fuco] + 1.41 [per]) / ΣDPw --- (3)

f_{nano} = (1.27 [19'HF] + 0.35 [19'BF] + 0.60 [allo]) / ΣDPw ---(4)

f_{pico} = (1.01 [chl *b*] + 0.86 [zea]) / ΣDPw --- (5)

where f_{micro}, f_{nano} and f_{pico} denotes fractions of micro-, nano- and pico- planktons contributing to the total phytoplankton biomass.

3. Results

3.1. *Spatial variations in hydrographic properties*

Our cruise encountered a well-developed anti-cyclonic eddy (ACE) (stations 25-45) north of 14^{o}N and a weaker ACE (ACE_w; stations 66-73) in the southwestern BoB (Fig. 1). The northwestern BoB was influenced by cyclone *Madi* (CM) associated with a cyclonic eddy (CE) (stations 47-55) offshore of the equatorward East India Coastal Current and weaker CE in the central Bay (stations 14-23; Sarma et al., 2016; Fig. 1). Shallow thermoclines were found associated with CE relative to those in ACEs (Figs. 2a). Similarly, the depth of the 26 ^{o}C isotherm was shallower (~55 m) in CE region and deeper (~85 m; t_{stat}=-27.7; $p<0.001$) in ACE region. The second half of the cruise (>2500 km along track distance) took place after the development of cyclone *Madi* in the western BoB. The stratification in the upper ocean was reduced relative to conditions prior to the onset of *Madi* (Fig. 2b). The water column density structure suggests that the 22 sigma-t isopycnal layer was shallower (40 m) in CE region that deepened to ~95 m in ACE in the north. Shallowing of 22 sigma-t to 40 m was observed again in the cyclone-influenced region (Fig. 2c).

The concentration of nitrate in surface waters, measured colorimetrically, was higher in the CE than in the ACEs (Table 1) and at several stations the concentrations were low (<0.1 □M) and close to detection limits (Fig. 3b).. The depth of nitracline, along the cruise track ranged between 26 and 80 m, deepening in ACEs and shoaling in the CE regions (t_{stat} = -9.04; $p<0.005$). Over all, the depths of nitracline coincided with those of thermocline (26 ^{o}C isotherm) and pycnocline (22 sigma-t isoline) in the entire study region (Figs. 2a and c). A significant linear correlation was observed between the depth of the nitracline and pycnocline (r^2 = 0.89; $p<0.001$) or thermocline (r^2 = 0.92; $p<0.001$). The mean concentration of phosphate in the surface waters was 0.13±0.1 □M with relatively lower (<0.1 □M) concentrations within the ACE region (0.08 □M; Fig. 2c; Table 1). Dissolved silicate concentrations varied between 1.3 □M and 4.4 □M and relatively higher concentrations (>2 □M) were found in the CE and ACEs. It was < 2 □M in the weaker ACE(ACE_w) and the cyclone-influenced region (Fig. 3d; Table 1) where silicate concentrations were well below the limiting levels (< 2 □M; Hatsun et al., 2017) in the mixed layer (Fig. 3d; Table 1) .

3.2. *Spatial variations in phytoplankton biomass and pigment signatures*

The vertical structure of Chl-*a* along the cruise track shows lower Chl-*a* values in the upper 20 m with persistent occurrence of subsurface Chl-*a* maxima (SCM) in the entire study region (Fig. 4a). Relatively higher Chl-*a* was observed in the cyclone-influenced region than in other regions in the upper 20 m (stations 47-55; t_{stat} = 2.04; $p<0.01$). The depth of SCM coincides with both thermocline (26^{o}C isotherm) and pycnocline (22 sigma-t) indicating that physical mixing has a significant impact on variations in Chl-*a* (Figs. 2a,c and 4a).

Among the accessory pigments, zeaxanthin (marker pigment for Cyanophyceae) concentrations were higher within the mixed layer (0.06 to 0.11µg l^{-1}), than chlorophyll-*b* (Chlorophyceae) and hexa-fucoxanthin (19' HF; Prymnesiophytes) (Figs. 4b-d). Fucoxanthin (Bacillariophyceae) and peridinin (Dinophyceae) concentrations were very low in the study region (data not shown). Relatively higher concentration of 19'HF and chlorophyll-*b* were observed in the CE (0.06 and 0.05 mg m^{-3} respectively) compared to ACE region (0.01 and 0.02 mg m^{-3} respectively; t_{stat} = 2.37; $p<0.05$) and statistically insignificant variations were observed for zeaxanthin (0.07 and 0.09 mg m^{-3} respectively; Figs. 4b-d). The distribution of phytoplankton size classes showed that micro-plankton communities were low and contributed between 10% and 15% whereas nano- and pico-plankton contributed 20-40% and 50-75% respectively (Figs. 5a-c). Relatively higher contribution of micro-plankton was observed in the CE (0.15) compared to ACE region (0.08; t_{stat} = 2.5; $p<0.01$). Overall, pico-plankton contribution dominated in the entire study region (Fig. 5c).

3.3. *Content and isotopic composition of particulate organic carbon and nitrogen*

In the marine environment, phytoplankton, zooplankton, bacteria and detritus are the main contributors to particulate organic matter (POM). The concentration of suspended particulate nitrogen (PN) and particulate organic carbon (POC) in surface waters of the study region varied from 0.4 to 1.7 □M and 3.4 to 12.1 □M respectively (Figs. 6a and b). Lower concentrations of both POC and PN were observed in the cyclone-influenced region and in the ACEs compared to the CE (t_{stat} = 2.47; $p<0.01$; Table 1). The mixed layer Chl-*a* displayed a significant linear correlation with POC (r^2 = 0.61; $p<0.001$; Fig. 7a) and PN (r^2 = 0.48; $p<0.001$; Fig. 7b) while neither POC nor PN displayed a significant correlation with salinity (Figs. 7c and d). The mean POC:Chl-*a* ratio was 178±58 in the study region. The POC:PN ratios varied between 5.7 and 9.4 (Fig. 6c) with a mean value of 6.9±0.8 which is close to Redfield ratio of 6.6 (Redfield, 1963).

The isotopic composition of POC (□$^{13}C_{sus}$) ranged between -26.3‰ and -24.1‰ in the regions of CE, cyclone-influenced (-25.0‰) and ACE (-24.7‰; Table 1). The variation in □$^{13}C_{sus}$ is within the range expected from pelagic planktons sources (Krishna et al., 2018). The □$^{13}C_{sus}$ displayed a linear relation with POC (r^2 = 0.52; $p<0.001$; Fig. 7e) indicating that higher production of phytoplankton leading to fixation of heavier dissolved inorganic carbon (DIC). The isotopic composition of PN (□$^{15}N_{sus}$) ranged from 1.8‰ to 6.3‰ (Fig. 6e) and displayed inverse relationship with PN (r^2 = 0.29; $p<0.05$; Fig. 7h). The range of □$^{15}N_{sus}$ in this study is consistent with the earlier studies (2.9-7.5‰; Saino and Hattori, 1980; 2.1 to 7.8 ‰; Kumar et al., 2004; 2005). In order to examine the influence

of river discharge on POC, PN, $\delta^{13}C_{sus}$, and $\delta^{15}N_{sus}$, these were plotted against salinity that revealed very poor relation in the study region (Fig. 7c-f).

4. Discussion

4.1. *Variability in $\delta^{13}C_{sus}$ and $\delta^{15}N_{sus}$ and sources of POC and nutrients in the BoB*

The concentrations of PN (0.4 to 1.7) and POC (3.4 to 12.1) in the suspended matter are within the range expected in the marine environment (Aumont et al., 2017). The POC:PN ratio ranged between 5.7 and 9.4 with a mean (SD) value of 6.9 (±0.8), which is close to Redfield ratio of 6.6, suggesting that *in situ* production contributed to POM pool in the study region. The POC:Chl-*a* (wt:wt) ratio can be used to identify the source of organic matter (Cifuentes et al., 1988; Richard et al., 1997; Bentaleb et al., 1998) as it is relatively low in fresh organic matter. The POC:Chl-*a* ratio of fresh organic matter produced by marine phytoplankton varies from ~40 (Montagnes et al., 1994), <70 (Geider, 1987) <100 (Head et al., 1996), <140 (Thompson et al., 1992) to <200 (Parson et al., 1977; Cifuentes et al., 1988; Bentaleb et al., 1998) due to regional differences in temperature, irradiance, growth rate and species composition (Heath et al., 1990; Geider et al. 1998). The POC:Chl-*a* ratio also depends on the variable rates of decomposition of POC and Chl-*a*. If Chl-*a* decomposes at a greater rate than POC, then the ratio elevates. If the degradation has occurred correspondingly, low C:N ratio implies that either the original material is mostly planktonic or bacteria (Hedges et al., 1997). The low C:N ratios and mean POC:Chl-*a* ratio of 178±58 suggest that POM is mainly produced *in situ*. This is further evidenced from the significant relation of both POC and PN with Chl-a (Figs. 7a, b). On the other hand, some fraction of terrestrial organic matter may be expected during summer monsoons in the BoB due to peak river discharge (June to September) associated with heavy precipitation over Indian subcontinent (Unger et al., 2003). It has been shown that terrestrial organic matter is mainly restricted to the shelf region or extends to a maximum of ~100 km offshore due to rapid sinking in association with river-borne mineral particles (Ittekkot et al., 1991). Kumar et al. (2004a; 2010) observed significant contribution of organic matter from terrestrial sources in the BoB during September-October 2002 when discharge from Ganges and Brahmaputra is at its peak. They noticed that the $\delta^{15}N_{sus}$ values were in the range of 2‰ to 3‰ at salinity <26 in the coastal western BoB and suggested significant contribution from terrestrial sources in the northern BoB. Despite the observed low saline waters (S = ~31) in the northern BoB, within ACE region, neither lower $\delta^{15}N_{sus}$ nor lower $\delta^{13}C_{sus}$ was observed in our study. In addition to this, the POC and PN and their isotopic compositions did not display a significant relationship with

salinity (r^2 = 0.02 p>0.1; Figs. 7c, d) suggesting that river water is not a source of POM in the study region.

Both $\delta^{13}C_{sus}$ and $\delta^{15}N_{sus}$ can be used as potential tracers to identify the major sources (marine *versus* terrestrial) of POM (Minagawa and Wada, 1986; Kumar et al., 2004a; Faganeli et al., 2009; Maya et al., 2011; Sarma et al., 2014; Krishna et al., 2014). The POM derived from marine and terrestrial sources contain distinctly different $\delta^{13}C$ and $\delta^{15}N$ signatures due to the differences in their inorganic carbon and nitrogen sources, respectively. The $\delta^{13}C_{sus}$ derived from terrestrial land plants of C_3 type is lower (-30 to -25‰; Middelburg and Nieuweuwenhuige, 1998; Barth et al., 1998) than marine phytoplankton (-24 to -18‰; Peters et al., 1978; Fry and Sherr, 1984; Middelburg and Nieuweuwenhuige, 1998; McMahon et al., 2013), but terrestrial plants of C_4 type have significantly higher values (-17 to -9‰; Smith and Epstein, 1971; Sackett, 1989). Similarly, $\delta^{15}N$ is significantly different with a range of terrestrial values of 1.8 to 3.0‰ (Peters et al., 1978; Wada et al., 1987; Thornton and McManus, 1994) and 5-8‰ (Altabet, 1996; Brandes and Devol, 2002; Lamb et al., 2006) for marine sources. The $\square^{13}C_{sus}$ and $\square^{15}N_{sus}$ in the BoB ranged from -26.3 to -24.1‰ and 3.2 to 6.3‰ (except for station 3 for $\square^{15}N_{sus}$ as it is ~1.8‰). $\square^{13}C_{sus}$ was slightly lower than expected from marine sources. Such lower $\square^{13}C_{sus}$ values could be due to an assimilation of dissolved inorganic carbon (DIC) from rivers. Growth rate of phytoplankton is also an important parameter that determines the $\square^{13}C_{sus}$ as high growth rate can lead to limited diffusion leading to higher $\square^{13}C$ values in the organic matter formed while low growth rates allow full expression of enzymatic fractionation resulting in lower $\square^{13}C$ values in the organic matter. Phytoplankton growth rate data were not available for this study period and hence its impact could not be evaluated. The surface waters of BoB are 2-3 units less saline than adjacent Arabian Sea and southern Indian Ocean due to input of freshwater from the rivers (Rao et al., 1994). Since $\square^{13}C_{DIC}$ of freshwater is significantly lower (-12 to -10‰) than marine DIC (0±2‰), the mixing with freshwater may decrease $\square^{13}C_{DIC}$ in the BoB (Chanton and Lewis, 1999; Kanduc et al., 2007). $\square^{13}C_{DIC}$ ranges between -4 and -1‰ in the BoB, with lower values in the coastal region, and it is 2-3‰ lower compared to the Arabian Sea and the south Indian Ocean (+1 to -1‰; our unpublished data). Therefore, the assimilation of lighter DIC by phytoplankton could have decreased $\square^{13}C_{sus}$ in the BoB (Popp et al., 1999). The linear relationship between $\square^{13}C_{sus}$ and POC (r^2 = 0.52; p<0.001; Fig. 7e) suggests that higher production of phytoplankton leading to fixation of heavier DIC resulting in increase in $\square^{13}C_{sus}$ and *vice versa*. This could be one of the potential reasons for variations in $\square^{13}C_{sus}$ in the BoB. Based on the C:N, and POC:Chl-a ratios, the relations between POC/PN and Chl-a, and isotopic composition of POC

and PN, and insignificant relation of salinity with POC/PN content and isotopic composition, we conclude that POM is mainly contributed by *in situ* processes during study period in the BoB.

The $\delta^{15}N_{sus}$ reflects the sources of nitrogen in the euphotic zone (Saino and Hattori, 1980). Trophic processes, however, modify its signatures. For instance, microbial decomposition of organic matter increases $\delta^{13}C_{sus}$ and $\delta^{15}N_{sus}$ values as well as POC:PN ratio (Hedges et al., 1997). Low $\delta^{15}N_{sus}$ values (3.2±0.8‰) (Fig. 6e and Table 1) were associated with deeper nitracline, and ACE in the northern BoB. If the nitracline is deep, phytoplankton has to rely on regenerated nutrients, and excretory products of heterotrophs, which have low $\delta^{15}N$ values compared to their body (Checkley and Entzeroth, 1985 and Checkley and Miller, 1986). As a result, the phytoplankton biomass produced by assimilation of these nitrogenous nutrients decreases the $\delta^{15}N_{sus}$ values. When there is very little new nitrate input into the system, the regenerated nitrogen within the euphotic zone becomes lower as the removal of heavier isotopes continues by sinking of dead heterotrophic biomaterial and faecal pellets (Saino and Hattori, 1980). The lesser the new nitrogen supply from deep water to the photic zone, the more isotopically depleted bioavailable nitrogen pool. On the other hand, supply of nitrogen through atmospheric deposition and nitrogen fixation, riverine nutrient supply and uptake of dissolved organic nitrogen (DON) could also deplete $\delta^{15}N_{sus}$ in the BoB. The phytoplankton composition, measured under the microscope, did not reveal occurrence of nitrogen fixers (*Trichodesmium sp.*) during the study period (Our unpublished data) suggesting that nitrogen fixation may not be a important causative factor for lower $\delta^{15}N_{sus}$ values. Hedge et al. (2008) noticed N_2 fixers, *Trichodesmium sp.,* in the southwestern BoB during winter and spring. Though we did not observe N_2 fixers during sampling period, it might have occurred prior to our sampling period and its signature might have remained in the suspended matter due to its longer residence time. N* (an indicator of nitrogen fixation following Gruber and Sarmiento, 1997) varies between 1.0 to 1.6 μM in the ACEs whereas lower (<0.3 to -1.2 μM) concentrations were observed in the other study region suggesting possible N_2 fixation in the ACEs. Recently, Krishna et al. (2016) estimated nutrients flux from the rivers to the BoB and found that only 5% of the riverine nutrients reach the coastal ocean and it is utilized within 15 km from the coast (Sarma et al., 2013). Prasad (2014) measured DON in the BoB and found its concentrations to be significantly higher than dissolved inorganic nitrogen. Therefore, it is possible that uptake of DON, in the absence of inorganic nitrogen, could lead to lowering $\delta^{15}N_{sus}$ in the ACE. The insignificant relationship between N* and $\delta^{15}N_{sus}$ suggest that depleted values of $\delta^{15}N_{sus}$ might not have caused alone by N_2 fixation and other possible mechanisms such as uptake of DON may also be possible. On the other hand, $\delta^{15}N_{sus}$ values in the CE and cyclone-influenced regions are comparatively higher (4.1 -

4.8‰) than ACE region (3.3-3.8‰; t_{stat} = 2.7; p<0.01; Table 1) associated with shallow nitracline and high salinity that enables continuous supply of subsurface nitrate to the euphotic zone. The mean $\square^{15}N_{sus}$ in the CE and cyclone-influenced region (4.5±0.7‰) is close to reported deep water $\square^{15}N$ values of nitrate in the BoB (5.5±0.5‰; Bristow et al., 2017). The much lower $\square^{15}N_{sus}$ value (~1.8‰) at station 3 was associated with high nitrate concentrations (1.6 □M) suggesting incomplete utilization of nitrate, as lighter $\square^{15}N_{No3}$ is preferred by phytoplankton, thus biomaterial formed will be depleted compared to the $\square^{15}N_{NO3}$ (Wada and Hattori, 1978). The relatively higher $\square^{15}N_{sus}$ in the CE and cyclone-influenced region is due to new nitrogen from deep water supporting primary production in these regions. In the ACE region regenerated nitrogen, DON uptake and N_2-fixation supported primary production during the study period.

4.3. *Spatial variations in f-ratios in the BoB*

The $\square^{15}N_{sus}$ shows a significant inverse relation with depth of nitracline (r^2 = 0.51; p<0.001; Fig. 8), indicating that the availability of subsurface nitrate mainly controlled the biological production in the BoB during the study period. We have excluded one point at station 45 between ACE and cyclone-influenced region where sharp increase in the depth of nitracline and moderate increase in Chl-a were noticed. The enrichment of $\square^{15}N_{sus}$ is probably due to partial utilization of nitrate, brought from the subsurface water.. In addition to this, the depth of nitracline showed significant inverse relation with POC (r^2 = 0.29; p<0.01) and PN (r^2 = 0.32; p<0.01) as the primary production in the mixed layer is governed by the depth of nitracline. Mino et al. (2002) found a significant relation between $\square^{15}N_{sus}$ and depth of nitracline in the Atlantic Ocean, and suggested that $\square^{15}N_{sus}$ reflects the source of nitrogen to the mixed layer. The slopes of relations between $\square^{15}N_{sus}$ and nitracline are almost similar in the Atlantic (0.047) and BoB (0.041). The intercept of the relation is also not statistically different in the Atlantic (5.7) and BoB (6.3; t_{test} = 8.9; p>0.1). The uniform intercept in both regions strongly indicate the robustness of the relationship which is mainly caused by uniform deep water $\square^{15}N_{NO3.}$ The slope between $\square^{15}N_{sus}$ and nitracline depth may be different in the Arabian Sea and equatorial Pacific where $\square^{15}N_{NO3}$ is higher due to occurrence of denitrification in the subsurface waters (Brandes et al., 1998). The shallow nitracline enhances nitrate input to the mixed layer and the suspended matter (phytoplankton), thus formed, will have higher $\square^{15}N_{sus}$ value. In contrast, deeper nitracline forces isotopically depleted regenerated nitrogen (ammonium) pool, possible N_2 fixation and DON uptake, to support primary production that will produce relatively low $\square^{15}N_{sus}$.

Assuming the nutrients requirement to the phytoplankton in the open-ocean region is supported by deep water mixing and regenerated nutrients, Mino et al. (2002) derived the following equation:

$\square^{15}N_{phyto} = f_{new:\,N} \times \square^{15}N_{new\,N} + (1- f_{new\,N}) \square^{15}N_{regen\,N}$ ..... (6),

where $f_{new:\,N}$ (dimensionless) is the fraction of production supported by new NO_3^- to the total primary production and $\square^{15}N_{phyto}$, $\square^{15}N_{newN}$, and $\square^{15}N_{regenN}$ (‰) are the isotopic compositions of phytoplankton, new NO_3^-, and regenerated NH_4^+, respectively (Mino et al., 2002). Here $f_{new:N}$ and $\square^{15}N_{regen:N}$ are estimated from their relationship to depth of nitracline (D_{NO3}) as follows:

$f_{new:N} = A / D_{NO3}$, ... (7)

$\square^{15}N_{regen:N} = \square^{15}N_{new\,N} - B^* D_{NO3}$ ..... (8)

where A and B are proportionality constants. The final relation shown below is obtained by combining all the above three equations.

$\square^{15}N_{phyto} = -B*D_{NO3} + (\square^{15}N_{new}\,N + A*B)$ ..... (9)

This equation could be compared with the observed inverse linear relation between $\square^{15}N_{sus}$ and nitracline depth, assuming that $\square^{15}N_{sus}$ is equal to $\square^{15}N_{phytoplankton}$ (Mino et al., 2002). The constants A and B are computed from the slope and intercept of the regression line (Fig. 8). Recently Bristow et al. (2017) measured $\square^{15}N_{NO3}$ in the BoB and found the mean deep water NO_3 to be ~5.5‰. This value is close to that of global average deep water nitrate isotopic ratio (5±0.6‰; Liu and Kaplan, 1989; Sigman et al., 1997). Though this value is measured in the northern BoB, it is assumed to be constant in the entire BoB due to absence of denitrification (Rao et al., 1994; Bristow et al., 2017; Sarma et al., 2016), which enriches this value. Hence, the $\square^{15}N_{new\text{-}N}$ in the BoB is used as 5.5‰ in the Equation 9. Values for A and B are calculated as 19.46 m and 0.041‰/m respectively, and the former is used to calculate the *f*- ratios from equation (7).

The estimated *f*-ratios varied from 0.23 to 0.70 in the study region with the average value of 0.40±0.14 (Table 1). Relatively low *f*-ratios were observed in the ACE region (0.27 ± 0.02) compared to CE region (0.41 ± 0.14). The *f*-ratios in cyclone *Madi* influenced region was slightly higher (0.54±0.12) than those in the CE region but the difference is statistically insignificant. The higher *f*-ratios in the CE and cyclone-influenced regions were associated with higher surface water nitrate (0.4 □M), compared to ACE region (0.1 □M). Therefore, a higher fraction of primary production seems to be exported from the euphotic zone in the CE region than in the ACE region. Our present estimation is consistent with the study of Vidya and Prasanna Kumar (2013) wherein the authors estimated enhanced biogenic fluxes by 42% in the CE region compared to non-eddy regions in the BoB. The spatial variations in *f*-ratios in the BoB are consistent with phytoplankton size distribution. Lower *f*-ratios are expected in regions dominated by picoplankton due to their smaller

size and their regeneration within the mixed layer. Though picoplankton dominates over the entire study region due to silicate limitation, higher micro-plankton contribution was noted in the CE and cyclone-influenced regions (14-15%) as a result of inputs of silicate from sub-surface waters. This is in contrast to that observed in the ACE region (~9%; Fig. 5). This indicates that spatial variations of *f*-ratio in the BoB are governed by nutrients input through physical mixing and modification of phytoplankton size distribution. The presently estimated mean *f*-ratio in the BoB (0.40±0.15) is lower than the earlier estimations using tracer incubation technique in the BoB (0.54-0.70; Kumar and Ramesh, 2005; Gandhi et al., 2010a) and Arabian Sea (0.52-0.82; Gandhi et al., 2010a). Chen et al. (1999) noticed wide variations in *f*-ratio in the East China Sea, which is influenced by upwelling of subsurface nutrients from Kuroshio Currents and Changjiang river discharge. Enhanced new production and *f*-ratios were observed in the upwelling region while new production in the river discharge region was controlled by other factors such as light, temperature. Higher *f*-ratios were observed (0.05 to 0.65) in the Crozet Plateau during austral summer (2004-2005) through seasonal changes in inorganic nutrient levels (Sanders et al., 2007). Similar values (between 0.39 and 0.86) were noticed in the Indian sector of the Southern Ocean (Mengesha et al., 1998; Goeyens et al., 1998). Bode et al. (2002) reported values of 0.39 to 0.42 in open-ocean situations in the Bellingshausen Sea and Gerlache strait, and a value of 0.64 in the western Bransfield strait (Table 2). Nevertheless, the estimated *f*-ratios using $\square^{15}N_{sus}$ in the BoB are lower than tracer incubation experiments as our method gives an integrated signal over the period of residence time of suspended matter in the mixed layer and avoids problems related to incubation, such as tracer recycling, incubation period etc. Therefore, isotopic composition of $\square^{15}N_{sus}$ could be a more reliable tracer to estimate integrated *f*-ratios in the mixed layer in regions.

Enhanced primary production in the CEs (Prasanna Kumar et al., 2004) and cyclones-influenced regions (eg: Madhu et al., 2002; Maneesha et al., 2011) were reported in the BoB. This study suggests that weaker stratification, formation of cyclonic eddies and vertical mixing by cyclones support higher new production, leading to increased export carbon flux. Chen et al. (2012) estimated that 525 CEs formed between 1992-2009 in the BoB with variable life spans (10-90 days) and sizes (10-800 km). If we assume all these CEs are highly productive, as was observed in this study, CEs could be an important contributor to the export flux of carbon in the BoB. While higher sinking carbon flux in the northern Bay may be attributed to mineral ballast during peak discharge (Ittekkot et al., 1991), the formation of CEs may be the main controlling factor in the south.

5. Conclusions

In this study, dominant oligotrophy was observed in the Bay of Bengal during November-December 2013, except in CE and cyclone-influenced regions where vertical mixing of water brought significant amount of nutrients to the mixed layer from the beneath. These nutrients supported the growth of phytoplankton in CE and cyclone-influenced regions. As a result, relatively higher contribution of microplankton was observed in the CE and cyclone-influenced regions whereas picoplankton and nano-plankton dominated in the remaining study region. The elemental ratios and isotopic composition of carbon and nitrogen of suspended matter suggest *in situ* processes contributed to organic matter production in the study region. Variations in nitracline depth are reflected in the $\delta^{15}N_{sus}$ in the surface waters, thus $\delta^{15}N_{sus}$ can be used as a proxy for the source of nitrogen. This study reveals that phytoplankton growth in the ACE is supported by nitrogen fixation, DON uptake and regenerated nitrogen.

The higher *f*-ratios observed in CE region (0.41±0.14) and cyclone-influenced region (0.54±0.12), compared to the ACE regions (0.27±0.06), point out the importance of mesoscale processes that elevate nutrients concentrations to the euphotic zone, and increase the exportable production from surface to deeper BoB. From this study, we conclude that the CEs would contribute greatly to the basin-wide primary and export productions in the Bay of Bengal. More observations and modelling studies are required to account for the contribution of CEs to the biological pump in the BoB.

Acknowledgements

We are thankful to the Scientist-in-Charge and the Director, CSIR-National Institute of Oceanography for their keen interest and encouragement. We are thankful to the ASIRI-OMM US-India collaboration supported by the Office of Naval Research (USA) and the Ministry of Earth Sciences (India). We thank the Captain and participants of cruise RR1317 on the R/V Roger Revelle for the measurements conducted. C.K. Sherin acknowledges CSIR/AcSIR for research fellowship. We would like to thank three anonymous reviewers and associate editor for their constructive criticism and suggestions.

References

Altabet, M.A. 1988. Variations in nitrogen isotopic composition between sinking and suspended particles: Implications for nitrogen cycling and particle transformation in the open ocean. Deep-Sea Res, I, 35, 535–554.

Altabet, M.A. 1996. Nitrogen and carbon isotopic tracers of the source and transformation of particles in the deep sea. In: Ittekkot V., Schaefer P., Honjo S. and Depetris P. J. (ed) Particle flux in the Ocean. SCOPE, Vol, 57, Wiley & Sons, Chichester, pp. 155-184.

Anand, S.., Rengarajan, R., Sarma, V.V.S.S., Sudheer, A.K., Bhushan, R., and Singh, S.K. 2017. Spatial variability of upper ocean POC export in the Bay of Bengal and the Indian Ocean determined using particle-reactive ^{234}Th. J. Geophys. Res: Oceans, 122, doi: 10.1002/2016JC012639.

Anand, S., Rengarajan, R., and Sarma, V.V.S.S. 2018. ^{234}Th based carbon export flux along the Indian GEOTRACES GI02 section in the Arabian Sea and the Indian Ocean**.** Global Biogeochem. Cycles, in press.

Asper, V.L., and Smith, W.O. 1999. Particle fluxes during austral spring and summer in the southern Ross Sea (Antarctica), J Geophys. Res., 104, 5345-5360.

Aufdenkampe, A.K., McCarthy, J.J., Rodier, M., Navarette, C., Dunne, J., Murray, J.W. 2001. Estimation of new production in the tropical Pacific. Global Biogeochem. Cycles, 15, 101-112.

Aumont, O., Hulten, M.V., Roy-Barman, M., Dutay, J.C.m, Ethe, Christian, and Gehlen, M. 2017. Variable reactivity of particulate organic matter in a global ocean biogeochemical model, Biogeosci., 14, 2321-2341.

Barth, J.A.C., Veizer, J., and Mayer, B. 1998. Origin of particulate organic carbon in the upper St. Lawrence: Isotopic constraints. Earth Plant. Sci. Lettrs, 162, 111-121.

Bender, M., Ducklow, H., Kiddon, J., Marra, J., and Martin, J. 1992. The carbon balance during the 1989 spring bloom in the North Atlantic Ocean, 27N, 20W. Deep-Sea Res., 39, 1707-1725.

Bentaleb, I., Fontugne, M., Descolas-Gros, C., Girardin, C., Mariotti, A., Pierre, C., et al. 1998. Carbon isotopic fractionation by plankton in the southern Indian Ocean: Relation between δ13C of particulate organic carbon and dissolved carbon dioxide. J. Mar. Syst., 17, 39–58. https://doi.org/10.1016/S0924-7963(98)00028-1.

Bode, A., Castro, c.G., Doval, M.D., Valela, M., 2002. New and regenerated production and ammonium regeneration in the western Bransfield Strait region (Antarctica) during phytoplankton bloom conditions in summer. Deep-Sea Res. II 49, 787–804.

Brandes, J.A., Devol, A.H., Yoshinari, T., Jayakumar, D.A, and Naqvi, S.W.A. 1998. Isotopic composition of nitrate in the central Arabian sea and Eastern Tropical North Pacific: a tracer for mixing and nitrogen cycles. Limnol. Oceanogr., 43, doi: 10.4319/lo.1998. 43.7.1680.

Brandes, J.A. and Devol, A.H. 2002. A global marine-fixed nitrogen isotopic budget: implications for Holocene nitrogen cycling. Global Biogeochem. Cycles, doi: 10.1029/ 2001GB001856.

Bristow, L.A., Callbeck, C.M., Larsen, M., Altabet, M.A., Dekaezemacker, J., Forth, M., Gauns, M., Glud, R.N., Kuypers, M.M.M., Lavik, G., Milucka, J., Naqvi, S.W.A., Pratihary, A., Revsbech, N.P., Thamdrup, B., Treusch, A.H., and Canfield, D.E. 2017. N_2 production rates limited by nitrite availability in the Bay of Bengal oxygen minimum zone, Nature Geosci., doi: 10.1038/NGEO2847.

Buesseler, K., Ball, L., Andrews, J., Beniteznelson, C., Belastock, R., Chai, F. and Chao, Y. 1998. Upper ocean export of particulate organic carbon in the Arabian Sea derived from thorium-234, Deep Sea Res., Part II, 45, 2461–2488.

Bunn, S.E., Longeragan, N.R., Kempster M.A., 1995. Effects of acid washing samples on stable isotope ratios of C and N inpenaeid shrimps and seagrass: implications for food web studies using stable isotopes. Limnol. Oceanogra., 40, 622-625.

Chanton, J.P., and Lewis, F.G. 1999. Plankton and dissolved inorganic carbon isotopic composition in a river-dominated estuary: Apalachicola Bay, Florida, Estuaries, 22, 575-583.

Checkley, D.M., Entzeroth L.C. 1985. Elemental and isotopic fractionation of carbon and nitrogen by marine, planktonic copepods and implications to the marine nitrogen cycle. J. Plank. Res., 7, 553-568.

Checkley, D.M., Miller C.A. 1986. Nitrogen isotopic fractionation by oceanic zooplankton. Eos Trans. AGU 67, 988.

Chen, Y.L.L., Lu, H.B., Shiah, F.K., Gong, G.C., Liu, K.K., Kanda, J. 1999. New production and f-ratio on the continental shelf of the East China Sea: Comparisons between nitrate inputs from the subsurface Kuroshio Current and the Changjiang River, Estuarine Coast Shelf Sci., 48, 59-75.

Chen, G., Wang, D., Hou, Y. 2012. The features and interannual variability mechanism of mesoscale eddies in the Bay of Bengal. Cont. Shelf Res., 47, 178-185.

Cifuentes, L. A., Sharp, J. H., and Fogel, M. L. 1988. Stable carbon and nitrogen isotope biogeochemistry in the Delaware estuary. Limnol. Oceanogra., 33, 1102–1115.

Coplen, T.B. 1996. New guidelines for reporting stable hydrogen, carbon and oxygen isotope-ratio data. Geochimca. et Cosmochimca. Acta 60, 3359-3360.

Emerson, S., Quay, P., and Wheeler, P.A. 1993. Biological productivity determined from oxygen mass balance and incubation experiments, Deep-Sea Res., 40, 2351-2358.

Emerson, S., Quay, P., Darl, D., Winn, C., Tupas, L., and Landry, M. 1997. Experimental determination of the organic carbon flux from open ocean surface waters. Nature, 389, 951-954.

Faganeli, J., Ogrinc, N., Kovac, N., Kukovec, K., Falnoga, I., Mozetic, P. and Bajt, O. 2009. Carbon and nitrogen isotope composition of particulate organic matter in relation tomucilage formation in the northern Adriatic Sea. Mar. Chem., 114, 102-109.

Fry, B. and Sherr, E. 1984. $\delta^{13}C$ measurements as indicators of carbon flow in marine and freshwater ecosystems. Cont. Mar. Sci., 27, 13–47.

Gandhi, N., Prakash, S., Ramesh, R., Kumar, S., 2010a. Nitrogen uptake rates and new production in the northern Indian Ocean. Indian J Mar. Sci., 39, 362-368.

Gandhi, N., Ramesh, R., Srivastava, R., Sheshshayee, M.S., Dwivedi, R.M., Raman, M., 2010b. Nitrogen uptake rates during spring in the NE Arabian Sea. International J Oceanogra. 127493.

Gauns, M., Madhupratap, M., Ramaiah, N., Jyothibabu, R., Fernandes, V., Paul, J.T., Prasanna Kumar, S., 2005. Comparitive accounts of biological productivity characteris tics and estimates of carbon fluxes in the Arabian Sea and Bay of Bengal. Deep-Sea Res., II 52, 2003-2017.

Geider, R.J. 1987. Light and temperature dependence of thee carbon to chlorophyll-a ratio in microalgae and cyanobacteria: implications for physiology and growth of phytoplankton, New Phytologist, 106, 1-34.

Geider, R. J., McIntyre, H. L., and Kana, T. M. 1998. A dynamic regulatory model of phytoplanktonic acclimation to light, nutrients, and temperature. Limnol. Oceanogr., 43, 679–694. https://doi.org/10.4319/lo.1998.43.4.0679.

Goering, J., Alexander, V., Haubenstock, N., 1990. Seasonal variability of stable carbon and nitrogen isotope ratios of organisms in a North Pacific Bay. Estuarine, Coastal and Shelf Sci. 30, 239-260.

Goeyens, L., Semeneh, M., Baumann, M.E.M., Elskens, M., Shopova, D., Dehairs, F., 1998. Phytoplanktonic nutrient utilisation and nutrient signature in the Southern Ocean. J. Mar. Syst., 17, 143–157.

Gomes, H.R., Goes, J.I., and Saino, T. 2000. Influence of physical processes and freshwater discharge on the seasonality of phytoplankton regime in the Bay of Bengal. Cont. Shelf Res., 20, 313-330.

Grasshoff, K., Ehrhardt, M., Kremling, K., (Eds.) 1983. Methods of Seawater Analysis, Verlag Chemie, Weinheim, pp. 89-224.

Gruber, N and J.L. Sarmiento, 1997. Global patterns of marine nitrogen fixation and denitrification, Global Biogeochem. Cycles, 11, 235-266.

Hatsun, H., Azetsu-Scott, K., Somavilla, R., Remy, F. et al. 2017. The sub-polar gyre regulates Si concentratiosn in the North Atlantic. Sci. Rep., 7, doi: 10.1038/s41598-017-14837-4.

Head, E.J.H., Harrison, W.G., Irwin, B.I., Horne, E., Li. W.K.W. 1996. Plankton dynamics and carbon flux in an area of upwelling off the coast of Morocco. Deep-Sea Res., I, 43, 1713-1738.

Heath, M. R., Richardson, K., and Kiørboe, T. 1990. Optical assessment of phytoplankton nutrient depletion. J. Plank. Res., 12, 381–396. https://doi.org/10.1093/ plankt/12.2.381

Hedges, J.I., Keil, R.G., Benner R., 1997. What happens to terrestrial organic matter in the ocean?. Organic Geochem., 27, 195-212.

Hedge, S., Anil, A.C., Patil, J.S., Mitbavkar, S., Venkat, K., Gopalakrishna, V.V. 2008. Influence of environmental settings on the prevalence of Trichodesmium spp. in the Bay of Bengal. Mar. Ecol. Prog. Ser., 356, 93-101.

Ittekkot, V., Nair, R.R., Honjo, S., Ramaswamy, V., Bartsch, M., Manginini, S., Desai, B.N., 1991. Enhanced particle fluxes in Bay of Bengal induced by injection of fresh water. Nature 351, 385–387.

Jahnke, R.A. 1996. The global ocean flux of particulate organic carbon. A real distribution and magnitude. Global Biogeochem. Cycles, 10, 71-88.

Kanduc, T., Szramek, K., Ogrinc, N., and Walter, L.M. 2007. Origin and cycling of riverine inorganic carbon in the Sava River watershed (Slovenia) inferred from major solutes and stable carbon isotopes. Biogeochem., 86, 137-154.

Krishna, M.S., Naidu, S.A., Subbaiah, Ch.V., Gawade, L., Sarma, V.V.S.S., Reddy, N.P.C. 2014. Sources, distribution and preservation of organic matter in a tropical estuary (Godavari, India), Estuaries and Coasts, doi: 10.1007/s12237-014-9859-5.

Krishna, M.S., Prasad, M.H.K., Rao, D.B., Viswanadham, R., Sarma, V.V.S.S., Reddy, N.P.C. 2016. Export of dissolved inorganic nutrients to the northern Indian Ocean from the Indian monsoonal rivers durng discharge period. Geochem. Cosmochem. Acta, 172-430-443.

Krishna, M.S., Mukherjee, J., Dalabehera, H.B., Sarma, V.V.S.S., 2018. Particulate organic carbon composition in temperature fronts of the northerneatern Arabian Sea during witner. J. Geophys. Res. Biogeosciences, 123, https://doi/org/10.1002/2018JG004387.

Kumar, S., Ramesh, R., Sardesai, S., Sheshshayee M.S., 2004a. High new production in the Bay of Bengal: Possible causes and implications. Geophys. Res. Lett. 31, L18304.

Kumar, S., Ramesh, R., Bhosle, N.B., Sardesai, S., Sheshshayee, M.S., 2004b. Natural isotopic composition of nitrogen in suspended particulate matter in the Bay of Bengal. Biogeosci. 1, 63-70.

Kumar, S., Ramesh, R., 2005. Productivity measurements in the Bay of Bengal using ^{15}N tracer: Implications to the global carbon cycle. Indian J Mar. Sci., 34, 153-162.

Kumar, S., Ramesh, R., Dwivedi, R.M., Raman, M., Sheshshayee, M.S., D'Souza, W., 2010. Nitrogen uptake in the northeastern Arabian Sea during winter cooling. International J Oceanogra., 819029.

Lamb, A.L., Wilson, G.P. and Leng, M.J. 2006. A review of coastal palaeoclimate and relative sea-level reconstructions using $\delta^{13}C$ and C/N ratios in organic material. Earth Sci. Rev., 75, 29-57.

Landry, M.R. barber, R.T., Bidigare, R.R., Chai, F., Coale, K.H., Dam, H.G., Lewis, M.R., Lindley, S.T., McCarthy, J.J., Roman, M.R., Stoecker, D.K., Verity, P.G., White, J.R. 1997. Iron and grazing constraints on primary production in the central equatorial Pacific: An EqPac synthesis. Limnol. Oceanogra., 42, 405-418.

Lee, Y.L., Lu, H.B., Shiah, F.K., Gong, G.C., Liu, K.K., and Kanda, J. 1999. New Production and F-ratio on the Continental Shelf of the East China Sea: Comparisons Between Nitrate Inputs From the Subsurface Kuroshio Current and the Changjiang River, Cont. Shelf Res., 48, 59-75.

Liu, K.K., Kaplan, I.R., 1989. The eastern tropical Pacific as a source of ^{15}N enriched nitrate in seawater off southern California. Limnol. Oceanogra., 34, 820-830.

Madhupratap, M., Gauns, M., Ramaiah, N., Prasanna Kumar, S., Muraleedharan, P.M., De Sousa, S.N., Sardessai, S., Muraleedharan, U., 2003. Biogeochemistry of the Bay of Bengal: physical, chemical and primary productivity characteristics of the central and western Bay of Bengal during summer monsoon 2001. Deep-Sea Res, II 50, 881-896.

Mariotti, A., 1983. Atmospheric nitrogen is a reliable standard for natural ^{15}N abundance Measurements. Nature, 303, 685-687.

Maya, M.V., Karapurkar S.G., Naik, H., Roy, R., Shenoy, D.M. and Naqvi, S.W.A. 2011. Intra-annual variability of carbon and nitrogen stable isotopes in suspended organic matter in waters of the western continental shelf of India. Biogeosci., 8, 3441-3456.

McCarthy, J.J., Garside, C., John L.N., 1999. Nitrogen dynamics during the Arabian Sea northeast monsoon. Deep-Sea Res, II 46, 1623-1664.

McMahon, K.W., Ling Hamaday, L. and Thorrold, S. R. 2013. A review of ecogeochemistry approaches to estimating movements of marine animals. Limnol. Oceanogra., 58, 697–714.

Mengesha, S., Dehairs, F., Fiala, M., Elskens, M., Goeyens, L., 1998. Seasonal variation of phytoplankton community structure and nitrogen uptake regime in the Indian Sector of the Southern Ocean. Polar Biol., 20, 259–272.

Middelburg, J.J., Nieuweuwenhuize, J., 1998. Carbon and nitrogen stable isotopes in suspended matter and sediments from the Schelde Estuary. Mar. Chem., 60, 217-225.

Minagawa, M. and Wada, E. 1986. Nitrogen isotope ratios of red tide organisms in the East China Sea: A characterization of biological nitrogen fixation. Mar. Chem., 19, 245-259.

Mino, Y., Saino, T., Suzuki, K., Maranon, E., 2002. Isotopic composition of suspended particulate nitrogen ($\square^{15}N_{sus}$) in surface waters of the Atlantic Ocean from 50^0 N to 50^0 S. Global Biogeochem. Cycles 16, 1059.

Montagnes, D. J. S., Berges, J. A., Harrison, P. J., and Taylor, F. J. R. 1994. Estimating carbon, nitrogen, protein and chlorophyll a from volume in marine phytoplankton. Limnol. Oceanogra., 39, 1044–1060. https://doi.org/10.4319/lo.1994.39.5.1044

Parson, T.R., Takahashi, M., Hargrave, B. 1977. Biological oceanographic Processes, 2nd ed. Pergamon.

Popp, B.N., Trull, T., Kenig, F., Wakeham, S.G., Rust, T.M., et al., 1999. Controls on the carbon isotopic composition of Southern Ocean phytoplankton, Global Biogeochem. Cycles, 13, 827-843.

Peters, K.E., Sweeney, R.E. and Kaplan, I.R. 1978. Correlation of carbon and nitrogen stable isotope ratios in sedimentary organic matter. Limnol. Oceanogra., 23, 598-604.

Pinnegar, J.K., Polunin, N.V.C., 1999. Differential fractionation of $\delta^{13}C$ and $\delta^{15}N$ among fish tissues: implications for the study of trophic interactions. Functional Ecol., 13, 225-231.

Prakash, S, Ramash, R., Sheshshayee, M.S., Mohan, R., Sudhakar, M. 2015. Nitrogen uptake rates and f-ratios in the Equatorial and Southern Indian Ocean. Curr. Sci., 108, 239-245.

Prasad, V.R. 2014. Variability in distribution of organic matter in Indian monsoonal estuaries and western coastal Bay of Bengal: Influence of river discharge and bacterial processes, Ph.D thesis, Andhra University, Visakhapatnam, India.

Prasanna Kumar, S., Muraleedharan, P.M., Prasad, T.G., Gauns, M., Ramaiah, N., De Souza, S.N., Sardesai, D.S., Madhupratap, M., 2002. Why is the Bay of Bengal less productive during summer monsoon compared to the Arabian Sea?. Geophys. Res. Lettrs, 29, 2235.

Prasanna Kumar, S., Nuncio, M., Narvekar, J., Kumar, A., Sardesai, S., De Souza, S.N., Gauns, M., Ramaiah, N., Madhupratap, M., 2004. Are Eddies nature's trigger to enhance biological productivity in the Bay of Bengal?. Geophys. Res. Lettrs, 31, L07309.

Rao, C.K., Naqvi, S.W.A., Kumar, M.D., Varaprasad, S.J.D., Jayakumar, D.A., George, M.D., and Singbal, S.Y.S. 1994. Hydrochemistry of the Bay of Bengal: Possible reasons for a different water-column cycling of carbon and nitrogen from the Arabian Sea. Mar. Chem., 47, 279–290.

Redfield, A. C., Ketchum, B. H., and Richards, F. A. 1963. The influence of organisms on the composition of seawater. In M. N. Hill (Ed.), The sea (Vol. 2, pp. 26–77). New York: Wiley.

Richard, P., Riera, P., and Galois, R. 1997. Temporal variations in the chemical and carbon isotope compositions of marine and terrestrial organic inputs in the bay of Marennes-Oléron, France. J. Coastal Res., 13, 879–899.

Sackett, W.M. 1989. Stable carbon isotope studies on organic matter in the marine environment. In: Fritz P. and Fontes J.C. (Eds.), Handbook of Environmental Isotope Geochemistry, Elsevier, New York, pp. 139-169.

Sambrotto, R.N., and Lorenzen, C.J. 1987. Phytoplankton and phytoplankton production in the coastal and oceanic areas of the Gulf of Alaska. In *The Gulf of Alaska: Physical Environmental and Biological Resources*, edited by D.W. Hood and S.T. Zimerman, pp. 249-282, U.S. Dep. Commerce, Washington, D.C.

Sanders, R., Morris, P.J., Stinchcombe, M. Seeyave, S., Venables, H. and Lucas, M. 2007. New production and the f-ratio around the crozet Plateau in austral summer 2004-2005 diagnosed from seasonal changes in inorganic nutrient levels. Deep-Sea Res. II, 54, 2191-2207.

Saino, T., Hattori, A., 1980. ^{15}N natural abundance in oceanic suspended particulate matter. Nature, 283, 752-754.

Sarma, V.V.S.S., Kumar, M.D., and Saino, T. 2006. Impact of sinking carbon flux on accumulation of deep-ocean carbon in the Northern Indian Ocean. Biogeochem., doi: 10.1007/s10533-006-9055-1.

Sarma, V.V.S.S., Krishna, M.S., Viswanadham, R., Rao, G.D., Rao, V.D., Sridevi, B., Kumar, B.S.K., Prasad, V.R., Subbaiah, Ch.V., Acharyya, T., and Bandopadhyay, D. 2013. Intensified oxygen minimum zone on the western shelf of Bay of Bengal during summer monsoon: Influence of river discharge, J. Oceanogra., 69, 45-55.

Sarma, V.V.S.S., Krishna, M.S., Prasad, V.R., Kumar, B.S.K., Naidu, S.A., Rao, G.D., Viswanadham, R., Sridevi, T., Kumar, P.P., Reddy, N.P.C. 2014. Distribution and sources of particulate organic matter in the Indian monsoonal estuaries during monsoon, J. Geophys. Res. (Biogeosciences), 11/2014,119, doi: 10.1002/2014JG002721.

Sarma, V.V.S.S., Rao, G.D., Viswanadham, R., Sherin, C.K., Salisbury, J., Omand, M.M. Mahadevan, A., Murty, V.S.N., Shroyer, E.L., Baumgartner, M., Stafford, K. 2016. Effects of freshwater stratification on nutrients, dissolved oxygen and phytoplankton in the Bay of Bengal. Oceanography, 29, 126-135.

Sigman, D.M., Altabet, M.A., Michener, R., McCorkle, D.C., Fry, B., Holmes, R.M., 1997. Natural abundance-level measurement of the nitrogen isotopic composition of oceanic nitrate: An adaptation of the ammonia diffusion method. Mar. Chem., 57, 227-242.

Smith, B.N. and Epstein, S. 1971. Two categories of $^{13}C/^{12}C$ ratios for higher plants. Plant Physiology (Bethesda) 47, 380-384.

Thompson, P.A., Guo, M., Harrison, P.J. 1992. Effects of variation in temperature. I. On the biogeochemical composition of eight species of marine phytoplankton, J. Phycology, 28, 481-488.

Thornton, S.F., McManus, J., 1994. Application of organic carbon and nitrogen stable isotope and C/N ratios as source indicators of organic matter provenance in estuarine systems: evidence from the Tay Estuary. Scotland. Estuarine, Coastal and Shelf Res., 38, 219-233.

Uitz, J., Claustre, H., Morel, A., Hooker, S.B., 2006. Vertical distribution of phytoplankton communities in open ocean: An assessment based on surface chlorophyll. J. Geophys. Res., 111, C08005.

Vidya, P.J., Prasanna Kumar, S., 2013. Role of mesoscale eddies on the variability of biogenic flux in the northern and central Bay of Bengal. J. Geophys. Res., Oceans 118, 5760-5771.

UNESCO, 1979. Discharge of selected rivers of the world, Paris.

Unger, D., Ittekkot, V., Schafer, P., Tiemann, J., and Reschke, S. 2003. Seasonality and interannual variability of particle fluxes to the deep Bay of Bengal: Influence of riverine input and oceanographic processes, Deep Sea Res., Part II, 50, 897–923.

Wada, E and Hattori, A. 1978. Nitrogen isotope effects in the assimilation of inorganic nitrogenous compounds by marine diatoms. Geomicrobiol. J, 1, 85-101.

Wada E., Minagawa M., Mizutani H., Tsuji T., Imaizumi R. and Karasawa K. 1987. Biogeochemical studies on the transport of OM along the Otsuchi River watershed, Japan. Estuarine Coastal Shelf Sci., 25, 321–336.

Wilkerson, F.P., Dugdale, R.C., and Barber, R.T. 1987. Effects of El Nino on new, regenerated, and total production in eastern boundary upwelling systems, J. Geophys. Res., 92, 14347-14353.

Figure 1: Study area depicting station locations overlaid on mean AVISO- sea surface height (cm) (color shading) and geostrophic currents (arrows) between 28 November and 12 December 2013. The cruise track along with station numbers is shown (white circles represent CTD stations and black circles water sampling stations). The track of cyclone *Madi* is drawn in red. The stations in ACE, CE and Cyclone-influenced regions are marked with blue boxes.

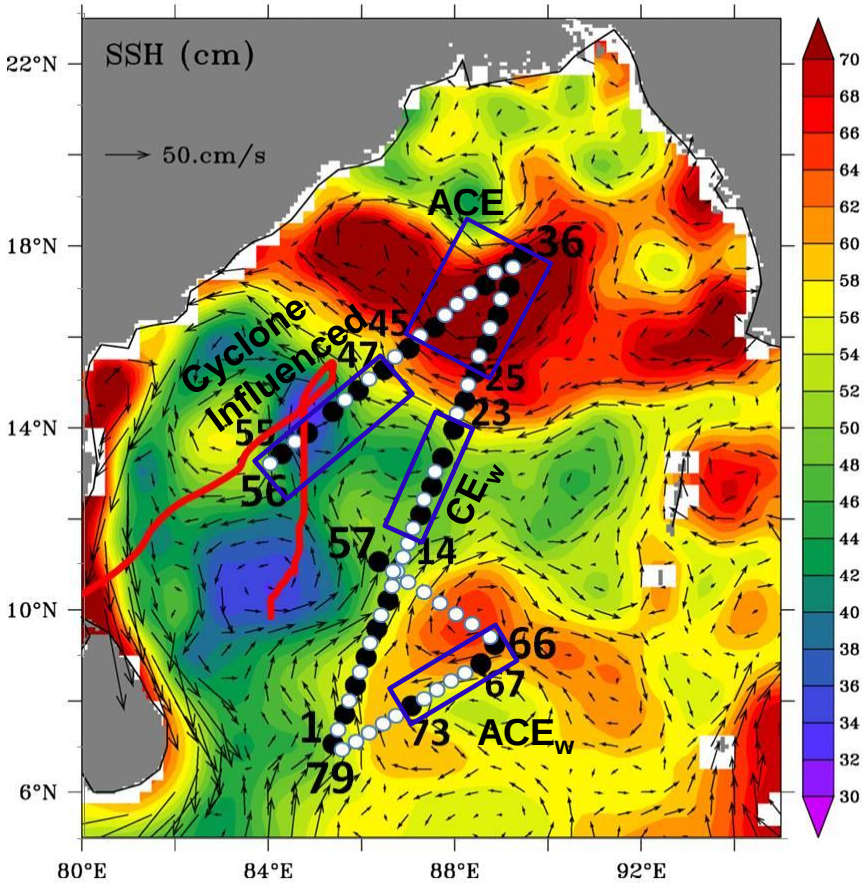

Figure 2: Depth-distance sections of a) temperature (^{0}C), b) salinity (psu) and c) density in the upper 100 m along the cruise track. The depth of the nitracline is also shown on all plots as a grey line. Station numbers are marked on the upper x-axis. Vertical dashed lines represent end of each transect shown in Figure 1.

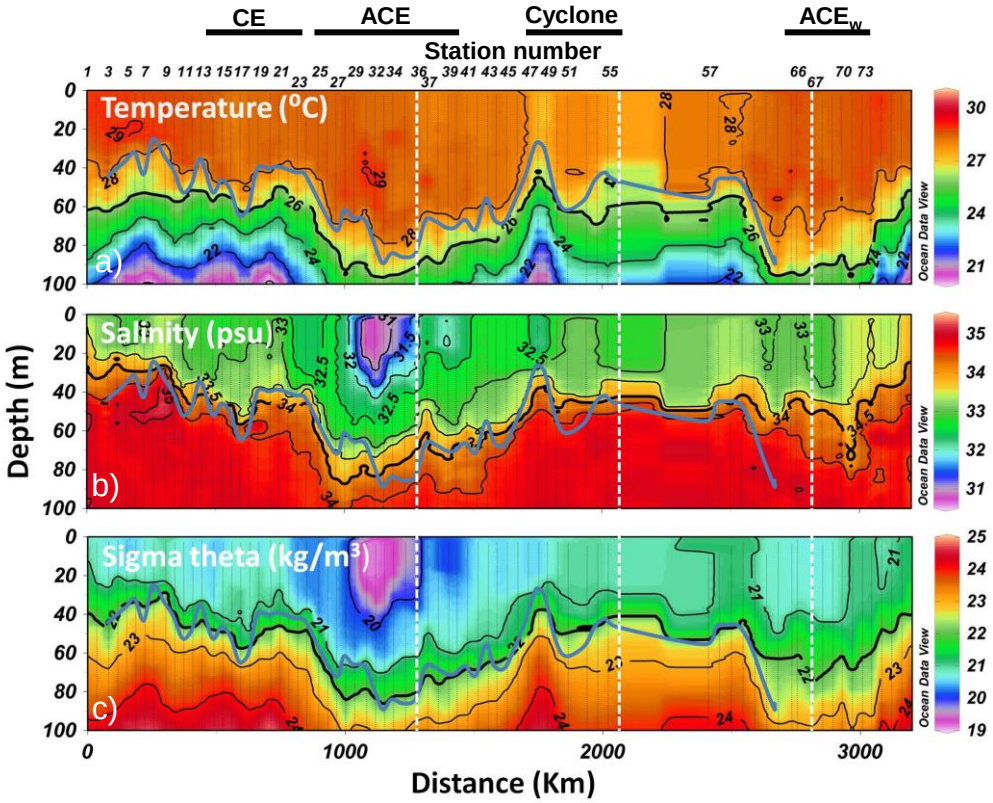

Figure 3: Depth-distance sections of a) ammonium (□M), b) nitrate (□M), c) phosphate (□M) and d) silicate (□M) along the cruise transect. The depth of the nitracline is also shown on the nitrate plot. Station numbers are marked on the upper x-axis. Vertical dashed lines represent end of each transect shown in Figure 1.

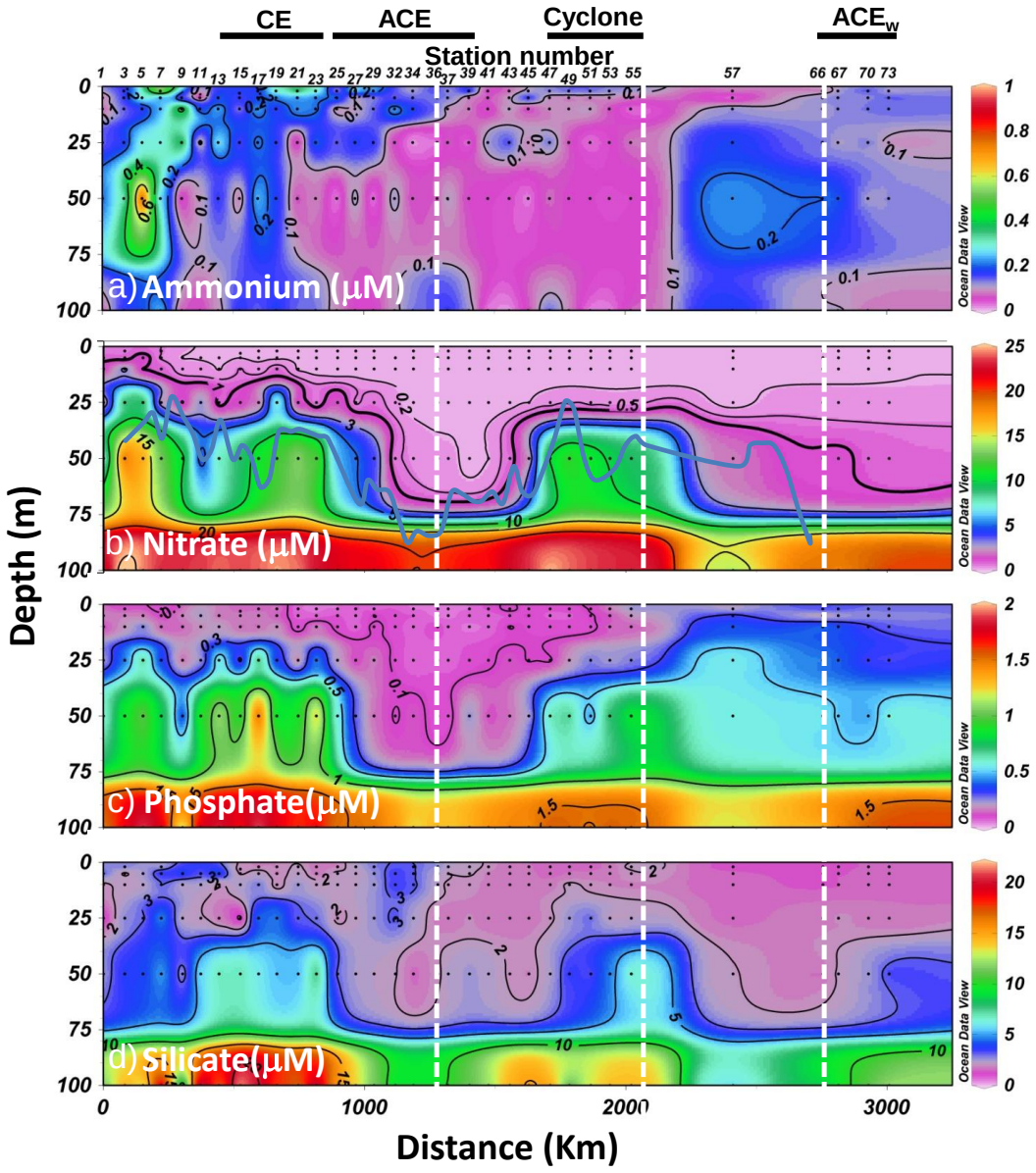

Figure 4: Sections of a) Chlorophyll-a (□g/L), b) Chlorophyll-b (□g/L), c) Hexa-fucoxanthin (□g/L) and d) zeaxanthin (□g/L) in the upper 80 m of the water column. Station numbers are marked on the upper x-axis. Vertical dashed lines represent end of each transect shown in Figure 1.

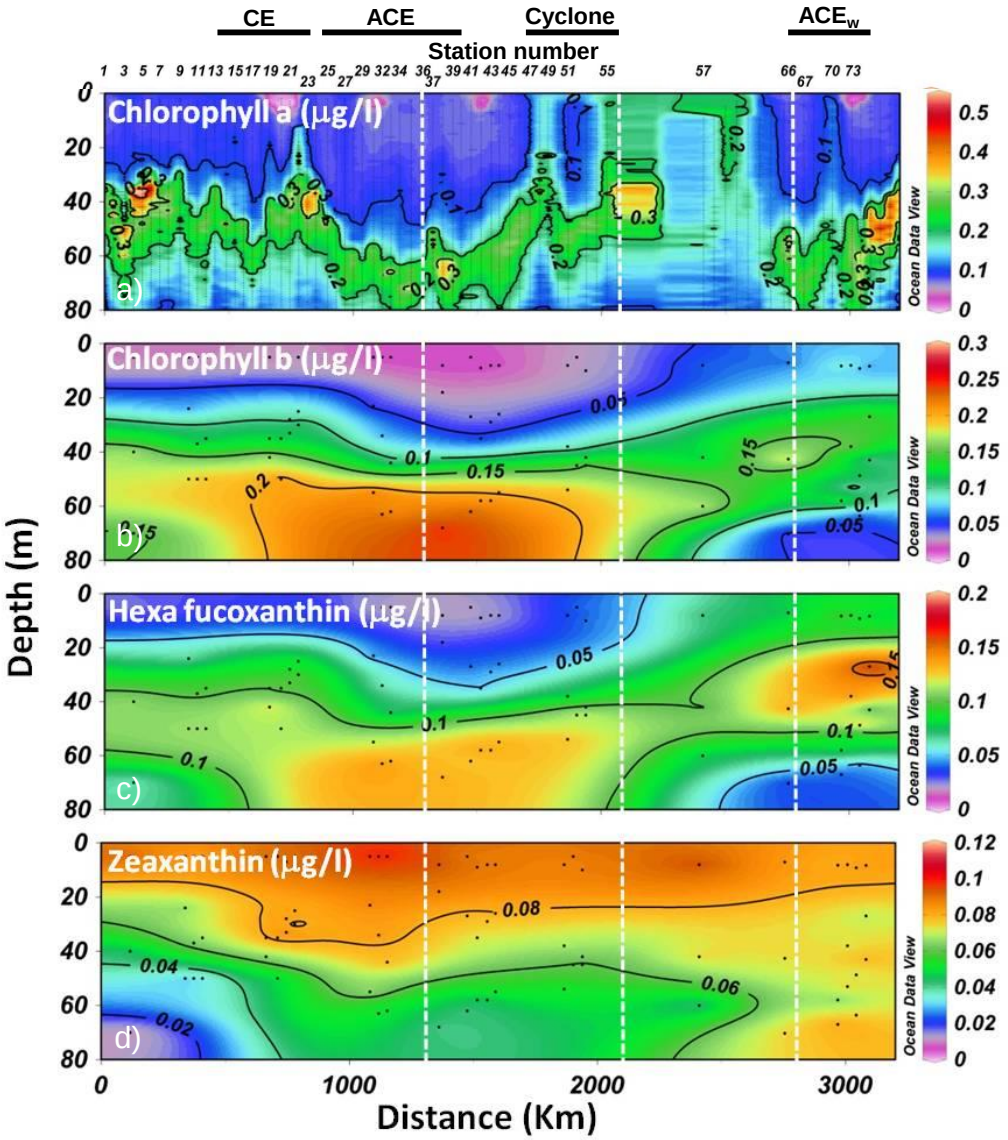

Figure 5: Sections of fraction of a) microplankton, b) nanoplankton and c) picoplankton in the water column. Station numbers are marked on the upper x-axis. Vertical dashed lines represent end of each transect shown in Figure 1.

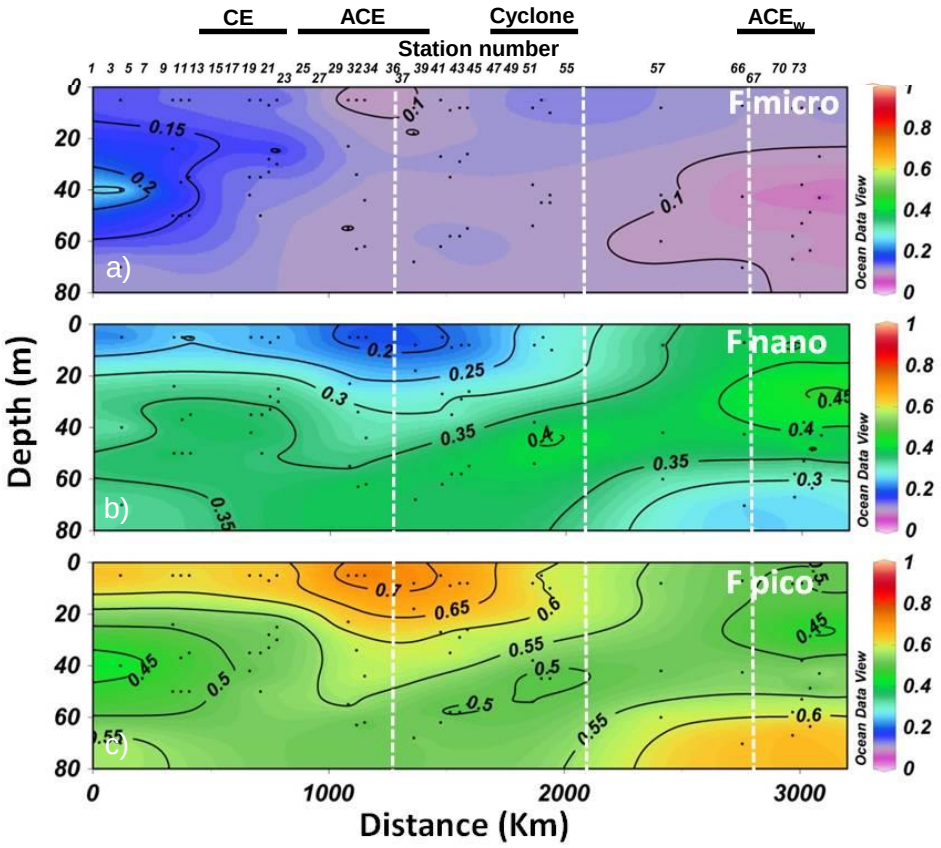

Figure 6: Variations in concentrations of surface POC, PN, POC:PN ratio, $\delta^{13}C_{sus}$, $\delta^{15}N_{sus}$ and *f*-ratios along the cruise track. Station numbers are marked on the upper x-axis.

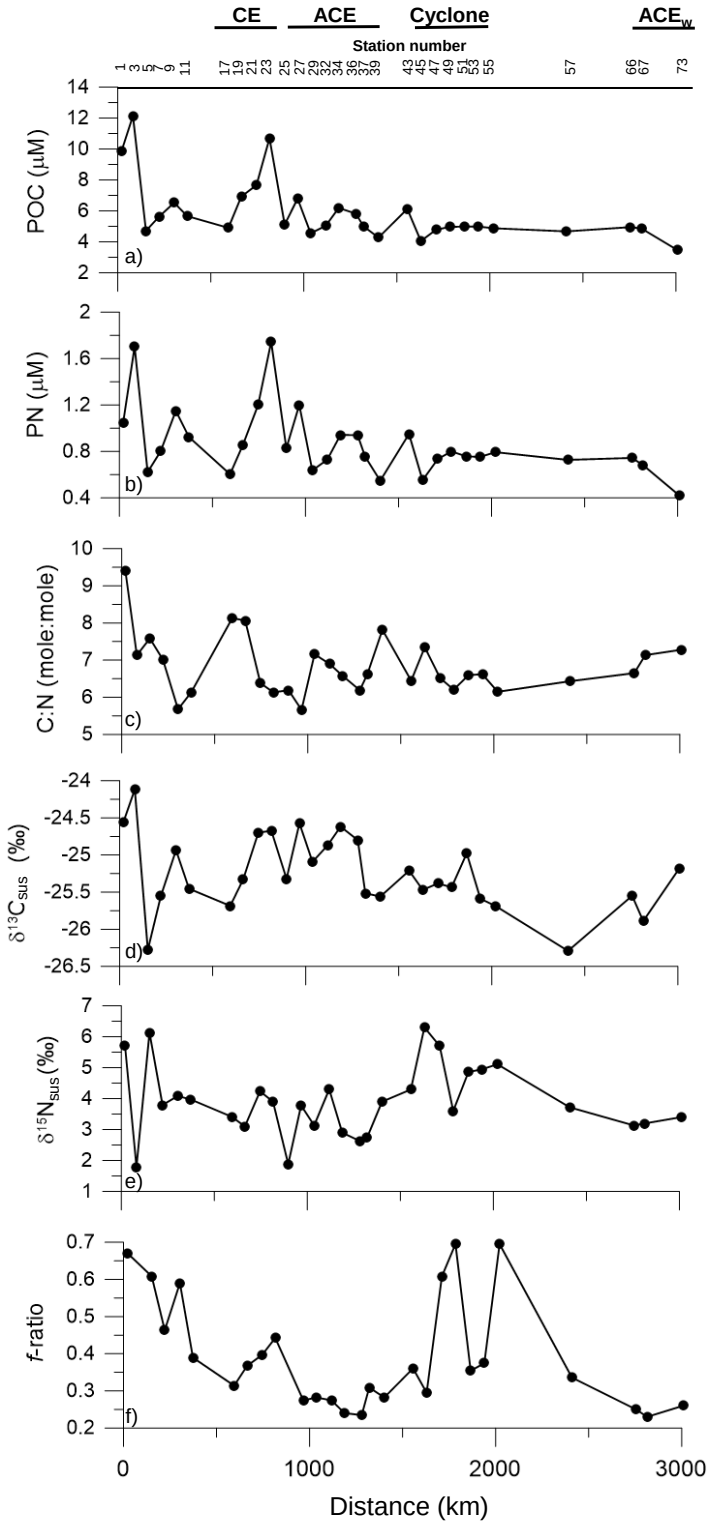

Figure 7: Correlations between Chlorophyll-a and a) POC,and b) PN; correlations between salinity and c) POC, d) PN, e) $\delta^{13}C_{sus}$, and f) $\delta^{15}N_{sus}$; (g) correlation between POC and $\delta^{13}C_{sus}$, and (h) correlation between PON and $\delta^{15}N_{sus}$.

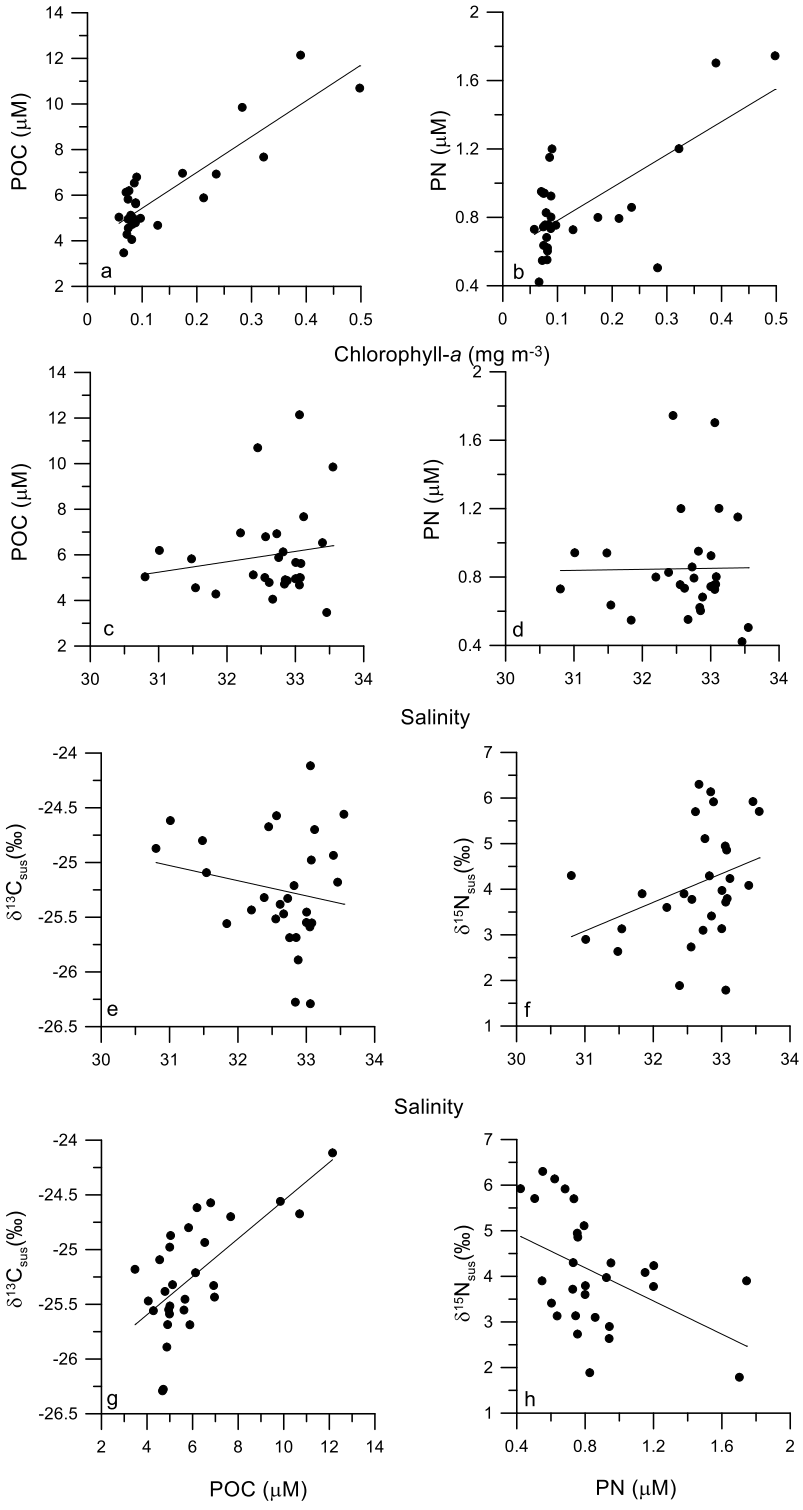

Figure 8: Scatter plot showing the relationship between depth of nitracline (m) and $\delta^{15}N_{sus}$ in the regimes of ACE (filled circles), Cyclone-influenced region (plus), CE (diamonds) and ACE_w (open circles). The point circled with dashed line was not considered while constructing regression equation as this point represents data collected from the boundary between ACE and Cyclone-influenced regions.

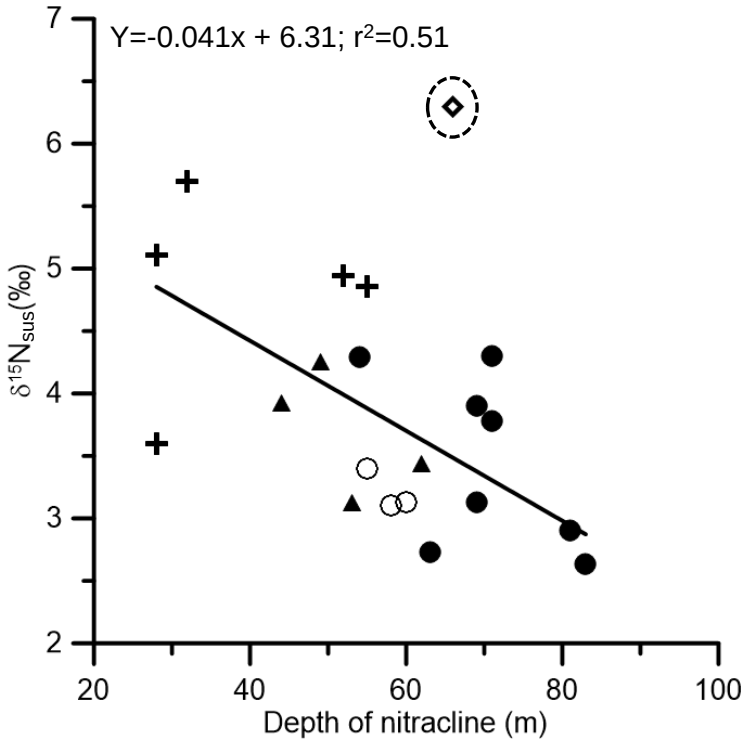

Table 1: Comparison of mean concentration of various biogeochemical properties in the mixed layer in the CE, ACE and Cyclone-influenced region

Regime	T (°C)	S(psu)	Chl-a	NO_3	PO_4	SiO_4	POC	PN	^{13}C	^{15}N	C/N	*f*-ratio
CE	28.34	32.86	0.12	0.69	0.18	2.14	7.5	1.1	-25.0	4.1	7.1	0.41
Cyclone	27.73	32.82	0.14	0.05	0.13	1.85	5.9	0.9	-25.4	4.8	6.4	0.54
ACE	28.29	32.0	0.07	0.11	0.07	2.23	4.9	0.7	-24.7	3.6	6.7	0.28
ACE (w)	28.58	33.25	0.08	0.14	0.28	1.54	4.0	0.5	-25.5	3.3	7.7	0.25

Table 2: *f*-ratios in various regions of world ocean estimated using different measurement techniques.

Oceanic Region	*f* -ratio	Method	Source
North Atlantic subtropical gyre	0.21 (0.14 – 0.33)	Stable isotopes	Mino et al. (2002)
South Atlantic subtropical gyre	0.16 (0.10 – 0.27)	Stable isotopes	Mino et al. (2002)
Equatorial Atlantic Ocean	0.30 (0.14 – 0.47)	Stable isotopes	Mino et al. (2002)
East China Sea	0.17-0.82	Geochemical	Lee et al.(1999)
Tropical North Pacific	0.01-0.46 (0.16±0.08)	Tracer incubation	Aufdenkampe et al. (2001)
Equatorial Indian Ocean	0.13-0.45	Tracer Incubation	Prakash et al. (2015)
Southern Ocean (Indian sector)	0.50	Tracer Incubation	Prakash et al.(2015)
Arabian sea (NE monsoon)	0.14 (± 0.08)	Tracer incubation	McCarthy et al. (1999)
North-eastern Arabian Sea (late NE monsoon)	0.26 (0.15 – 0.40)	Tracer incubation	Kumar et al. (2010)
Bellingshausen Sea	0.39	Tracer incubation	Bode et al. (2002)
Gerlache Strait	0.42	Tracer incubation	Bode et al.(2002)
Bransfield Strait	0.64	Tracer incubation	Bode et al.(2002)
Crozet Plateau	0.39-0.69	Tracer incubation	Mengesha et al. (1998)
Crozet Plateau	0.39-0.86	Geochemical	Goeyens et al. (1998)
Tropical Pacific	0.01-0.46	Tracer Incubation	Aufdenkampe et al. (2001)
Equatorial Pacific-Normal	0.12	Tracer incubation	Landry et al. (1997)
Equatorial Pacific-El Niño	0.07	Tracer incubation	Landry et al. (1997)
Ross Sea	0.68	Tracer incubation	Asper and Smith (1999)
Station P	0.42	Geochemical	Sambrotto and Lorenzen (1987); Emerson et al. (1993)
Peru-Normal	0.42	Tracer incubation	Wilkerson et al. (1987)

Peru-El Niño	0.30	Tracer incubation	Wilkerson et al. (1987)
North Atlantic Bloom Experiment	0.50	Tracer incubation	Bender et al., 1992
Arabian Sea (NEmonsoon)	0.15	Tracer incubation	McCarthy et al., 1999
North-eastern Arabian Sea (Pre-monsoon)	0.69 (0.52 – 0.82)	Tracer incubation	Gandhi et al. (2010b)
Bay of Bengal (Pre-monsoon)	0.70 ± 0.1	Tracer incubation	Gandhi et al. (2010a)
Bay of Bengal (Post-monsoon)	0.54 ± 0.22	Tracer incubation	Kumar and Ramesh (2005)
Bay of Bengal (Post-monsoon) : CE region	0.50 ± 0.16	Stable isotopes	Present study
Bay of Bengal (Post-monsoon) : ACE region	0.27±0.06	Stable isotopes	Present study